



# Drop impacting on a single layer of particles: Evolution of ring without particles

Cite as: Phys. Fluids 31, 047107 (2019); <https://doi.org/10.1063/1.5090909>

Submitted: 30 January 2019 . Accepted: 03 April 2019 . Published Online: 24 April 2019

Jianguen Zheng, Jiayan Li, Feng Tao, Lingjun Zhang, Yingzhou Huang , Shuxia Wang, and Guo Chen 



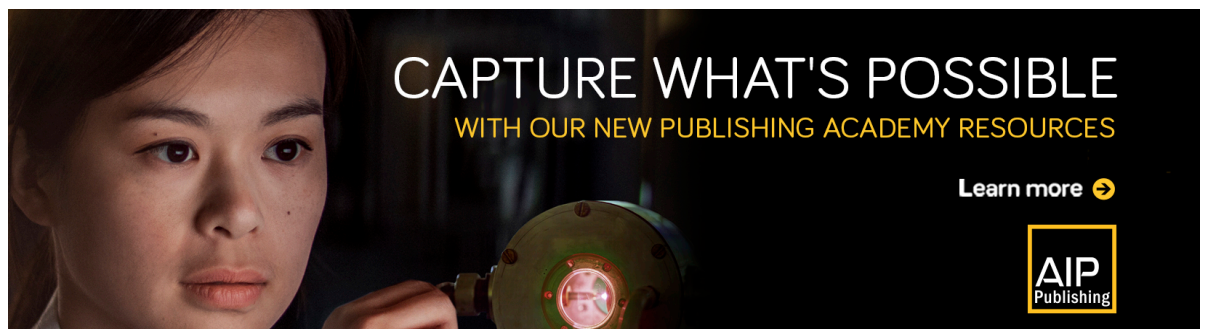
[View Online](#)




[Export Citation](#)





[CrossMark](#)



CAPTURE WHAT'S POSSIBLE  
WITH OUR NEW PUBLISHING ACADEMY RESOURCES

Learn more 



# Drop impacting on a single layer of particles: Evolution of ring without particles

Cite as: *Phys. Fluids* **31**, 047107 (2019); doi: [10.1063/1.5090909](https://doi.org/10.1063/1.5090909)

Submitted: 30 January 2019 • Accepted: 3 April 2019 •

Published Online: 24 April 2019



Jianguen Zheng, Jiayan Li, Feng Tao, Lingjun Zhang, Yingzhou Huang,<sup>a)</sup>  Shuxia Wang, and Guo Chen<sup>a)</sup> 

## AFFILIATIONS

Chongqing Key Laboratory of Soft Condensed Matter Physics and Smart Materials, College of Physics, Chongqing University, Chongqing 400044, People's Republic of China

<sup>a)</sup> Authors to whom correspondence should be addressed: [yzhuang@cqu.edu.cn](mailto:yzhuang@cqu.edu.cn) and [wezer@cqu.edu.cn](mailto:wezer@cqu.edu.cn)

## ABSTRACT

In this study, we examined the impacts of a millimeter sized water drop hitting a layer of uniformly distributed particles on a hydrophilic/hydrophobic glass slide. A ring/disc structure without particles was formed and modified by two mechanisms: pushout and pullback. The pushout factor dominated the process when the drop hit on the hydrophilic glass slide, while the pullback factor played a decisive role during impact on the hydrophobic surface. The rebound of a drop on the hydrophobic surface formed a disc-shaped ring. We showed that the ratio of the effects of these two factors on the ring/disc width were independent from the impact speed, in both experimental and scaling analyses. Our results also suggested that higher hydrophobicity of a water drop on the hydrophobic glass slide, instead of a polymethyl methacrylate (PMMA) particle surface, resulted in a lower maximum spreading distance when the drop hit the PMMA particle layer on a hydrophobic surface.

Published under license by AIP Publishing. <https://doi.org/10.1063/1.5090909>

## INTRODUCTION

The impacts of drops on solid substrates or liquid layers have been extensively studied for decades,<sup>1–4</sup> leading to the discovery of fascinating phenomena, from splashing<sup>5–8</sup> to rebounding.<sup>9</sup> Drop impacts are also technologically important in areas such as forensic science and blood splattering,<sup>10,11</sup> raindrop effects on soil hydrological and erosional processes,<sup>12,13</sup> and ink-jet printing routines.<sup>14–16</sup> With the development of new technology, more complex drops and sophisticated substrates have been designed, enriching our knowledge of drops impacts on varied surfaces.<sup>4,17–21</sup> Peters and his group<sup>22</sup> investigated the impacts of dense suspension drops onto a solid substrate and proposed a new energy balance to predict splash onset at the particle level in the suspension. Recently, Amirfazli *et al.*<sup>23</sup> found that the addition of particles to a water drop can change the impact and spread on hydrophilic and hydrophobic surfaces, possibly due to energy dissipation through frictional losses between particles and the substrate.

In addition to making the drops more complicated, changes to the substrate have also been made. Hao<sup>7</sup> found that a slightly roughness of substrate could significantly enhance corona splashing. Sivakumar and Vaikuntanathan<sup>24</sup> studied drop impacts on groove-textured surfaces and observed that the maximum drop spread

perpendicular to the grooves was always less than the spread parallel to the grooves. Zhao and his collaborators<sup>25</sup> explored drop impacts on a granular substrate using high-speed, double-laser profilometry measurements, and they classified the dynamics into three aspects: deformation of the substrate during impact, the maximum spread diameter of the drop, and penetration of the liquid into the substrate.

However, little attention has been paid to drop impacts on a monolayer of uniformly distributed particles, especially related to landform change after impact. Therefore, we directly observed and investigated the impact of a water drop on a single layer of polymethyl methacrylate (PMMA) particles with varied impact velocity using a high-speed camera. We found that an interesting, particle-free ring/disc shape appeared after impact via two mechanisms: pushout and pullback. The pushout factor played a main role during drop impact on the single layer of particles on a hydrophilic glass slide, while the pullback factor dominated when the surface is hydrophobic. This study generalizes and improves the understanding of drop impacts on complex surfaces.

## MATERIALS AND METHODS

In this study, we carefully explored the progress as a millimeter-sized water drop impacted a specially prepared glass slide, which

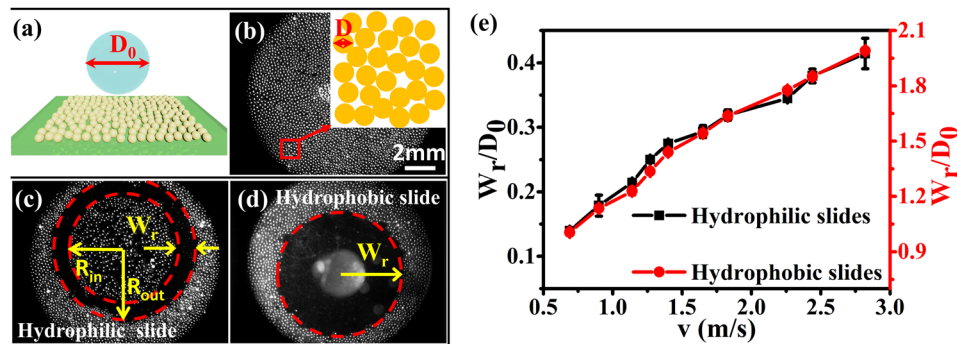


**FIG. 1.** (a) An illustration of the impact of a water drop with diameter  $D_0$  onto a single layer of particles. (b) The single layer of PMMA particles is viewed from the bottom, and the magnified inset shows the random close packing structure. (c) Ring-like structure from a drop hitting the particle layer on a hydrophilic glass slide.  $W_r$  is the width of the ring without particles.  $R_{in}$  and  $R_{out}$  indicate the inner and outer boundary of the ring, respectively. (d) Disc-like structure from a drop hitting a particle layer on the hydrophobic slide. Here,  $W_r$  stands for the radius of the disc and equals to  $R_{out}$ . (e) Representative plot of  $W_r/D_0$  vs  $v$  for hydrophilic (black square) and hydrophobic (red circle) surfaces.

was covered by a single layer of PMMA particles of diameter  $D$  ( $D = 75 \pm 1 \mu\text{m}$ ), as illustrated in Fig. 1(a). Figure 1(b) shows that PMMA particles were distributed uniformly and formed a random close packing structure. The experimental setup was mounted on a microscope (OLYMPUS IX73, Japan). A water drop with a diameter ( $D_0$ ) of  $3.12 \pm 0.10 \text{ mm}$  was pumped out from an injector controlled by a stepping motor (Longer Pump LSP01-2A, China). The pumping rate was set at a low value of  $50 \mu\text{l}/\text{min}$  to ensure the drop's free fall, i.e., the initial velocity of the drop was close to zero. The free-falling drop hit the target surface at velocities ranging from  $0.69 \text{ m/s}$  to  $2.82 \text{ m/s}$  by releasing the drop at different heights ranging from  $0.04 \text{ m}$  to  $0.5 \text{ m}$ . The impact speed was also verified from side view images and was consistent with the velocity formula  $v = \sqrt{gH_0(1 - \exp(-2(H - \Delta H)/H_0))}$  considering drop oscillation and air drag as indicated by Nicolas,<sup>26</sup> where  $g$  is the gravitational acceleration,  $H$  is the releasing height of drop,  $\Delta H$  is the distance between the syringe outlet and the drop at zero velocity, and  $H_0 = \frac{4\rho D_0}{3C_f \rho_{air}}$ , where  $\rho$  is the density of water,  $C_f$  is the constant friction coefficient,<sup>27</sup> and  $\rho_{air}$  is the density of air. We recorded the complete dynamic striking process and subsequent drop movement from the bottom using a high-speed camera (Phantom V7.3, Vision Research, Inc.) at a frame rate of  $5000 \text{ fps}$  to carefully inspect the interaction between the drops and particles. Two types of glass slides, hydrophilic and hydrophobic, were tested in the experiment. An untapped glass slide was used as the hydrophilic interface, and the hydrophobic slide was prepared by ultrasound cleaning a hydrophilic slide for  $10 \text{ min}$ , which then was treated with a commercial coating agent (Glaco Mirror Coat "Zero", Soft 99 Co.) containing nanoparticles and an organic reagent.<sup>28</sup>

## RESULTS AND DISCUSSION

Remarkably, we observed that a ring-like region without any particles appeared after the water drop impacted on the particle layer on a hydrophilic glass slide for all impact speeds in the experiment, as illustrated by red dashed lines in Fig. 1(c). The inner and outer contours of the ring are illustrated by red dashed lines.  $W_r$  ( $W_r = R_{out} - R_{in}$ ) is the width of the ring without particles.

The ring-like shape formed a disc when the slide was hydrophobic due to the full retraction and bounce of the drop after impact onto a hydrophobic substrate, leading to the disappearance of the ring inner radius, as shown in Fig. 1(d). Here  $W_r$  ( $W_r = R_{out}$ ) stands for the radius of the disc. However, the incomplete retraction of the drop on the hydrophilic surface limited the particle movement range and formed the inner radius of the ring.

It should be pointed out that both the width of the nonparticle ring on the hydrophilic surface and the radius of the disc without particles on the hydrophobic slide were defined as  $W_r$ . Figure 1(e) shows that  $W_r$ , normalized by  $D_0$ , increased with increasing impact velocity, as illustrated by the black squares (hydrophilic slide) and red circles (hydrophobic slide).

The high-speed images revealed the detailed dynamic formation of a nonparticle ring-like region for a drop impact velocity of around  $1.26 \text{ m/s}$  on the hydrophilic glass slide surface. As shown in Fig. 2(a), the drop touched the particle layer at  $0 \text{ ms}$ , and then pushed the particles outward as it spread across the surface at  $1 \text{ ms}$ . The origin and direction of the red arrows, respectively, mark the instantaneous position and direction of motion of the particles. The drop front illustrated by a solid red circle was coincident with the contour of moving particles during drop spread. The radius of drop front  $R$  is indicated by a yellow arrow and reached its maximum value ( $R_{max}$ ) at around  $4 \text{ ms}$ . Then, the drop began to retract and pulled back particles that were trapped inside the drop. At the same time, other particles that were not connected with the drop continued to move outward in the radial direction due to nonzero kinetic energy. The contours of moving particles are indicated by red dashed lines. At around  $60 \text{ ms}$ , all particles came to rest and those that were pulled back and pushed out formed the inner ( $R_{in}$ ) and outer ( $R_{out}$ ) boundaries of the ring, respectively.

These observations suggest that two mechanisms led to the formation of the nonparticle ring-like structure: one was controlled by the surface tension of drop and resulted in the formation of  $R_{in}$ . We quantitatively defined its contribution on the nonparticle ring/disc as the defined "pullback," where the pullback factor on the nonparticle ring/disc width was defined as  $W_{pullback}$  and  $W_{pullback} = R_{max} - R_{in}$ ; the other originated from the drop inertia and led to the formation of  $R_{out}$ . Its effect on the nonparticle ring/disc was

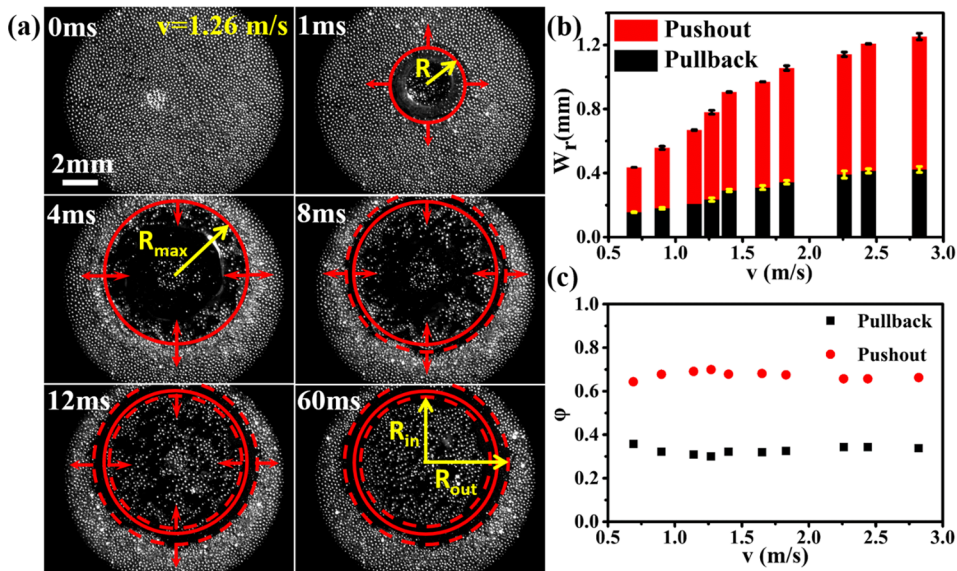


**FIG. 2.** (a) Corresponding high speed images show the formation of a non-particle ring-like structure when a drop impacts a single layer of particles distributed on the hydrophilic surface. (b) Plot of the ring width vs the drop impact velocity considering the contributions of two factors, and red and black bars are the contributions of pushout and pullback, respectively. (c) The ratio of each factor's influence on the ring width was plotted for various impact velocities. Red circles and black squares represent the ratios of pushout and pullback, respectively.

quantitatively defined as  $W_{pushout}$  and  $W_{pullback} = R_{out} - R_{max}$ . In addition, we have also defined the ratio of each factor's influence on the whole ring/disc width as  $\phi$ , and  $\phi = W_{pullback}/W_r$  or  $\phi = W_{pushout}/W_r$  showing the contribution of pullback or pushout factor, respectively. We have compared the contributions of these two factors to the ring-like structure width. Figure 2(b) shows ring width  $W_r$  as a relationship of the impacting velocity.  $W_r$  equals  $R_{out}$  minus  $R_{in}$  and is composed of two parts. The black bar refers to the pullback factor contribution, and the red bar represents the effect of the pushout factor. Although the effects of both factors on the ring width increased as the impact velocity rose, pushout played a main role in the formation of the nonparticle ring structure and contributed 60%–70% of the ring width within the velocity range of this experiment, as shown in Fig. 2(c).

One essential question remains unclear: why was the ratio almost constant throughout the experiment, instead of increasing with the impact velocity,  $v$ ? We propose the following explanation: the pushout factor effect increased to the velocity of outward-moving PMMA particles,  $v_p$ , which should be proportional to the expanding velocity of the drop on the substrate,  $v_e$ . As suggested by Xu,<sup>29</sup>  $v_e \propto v^{1/2}$ . We therefore obtain  $v_p \propto v_e \propto v^{1/2}$ . On the other hand, the pullback factor effect depended on the retraction velocity of a flattened drop on the substrate, which is defined as  $v_{re}$  and  $v_{re} = \sqrt{2\sigma/\rho h} \propto h^{-1/2}$  according to Varanasi's work,<sup>30</sup> where  $\sigma$ ,  $\rho$ , and  $h$  are the liquid-air surface tension, liquid density, and thickness of the flattened drop, respectively. The total volume of drop ( $V$ ) can be reasonably assumed to be unchanged during impact and expansion,  $V \cong \pi R_{max}^2 h$ . The maximum expanding radius of a drop follows the scaling law  $R_{max} \sim We^{1/4}$ ,<sup>25,31</sup> where  $We$  is the Weber number and  $We \sim \rho v^2 D_0 / \sigma$ . As a result, we have  $v_{re} \propto h^{-1/2} \propto R_{max} \propto We^{1/4} \propto v^{1/2}$ . Therefore, we finally obtain  $v_p \propto v_{re} \propto v^{1/2}$ , which proves that the ratio of each factor contribution on the right width was independent of the impact velocity.

When a drop impacted the hydrophobic surface, the situation was different and the pullback factor became more important.

Figure 3(a) shows the formation of a nonparticle disc when a drop impacted the particle layer on the hydrophobic slide. The drop hit the particle layer at 0 ms and pushed the particles outward to reach the maximum diameter at around 4 ms. Then, the drop retracted and drew the attached particles inward as indicated by red arrows. Other particles that were not attached to the drop kept moving outward along the radial direction. Moving particle profiles are also indicated by red dashed lines. When the particles that had been pushed out stopped moving at around 9 ms, the ones that were adhered to the drop did not come to rest and kept moving with the rebounding drop. At about 65 ms, the drop left the surface completely, causing the inner radius of ring to disappear and forming a nonparticle disc. The disc radius  $R_{out}$  depends on how far the particles can travel outward. Figure 3(b) shows the width of disc  $W_r$ , i.e.,  $R_{out}$  ( $R_{in}$  equals to zero), for different impact velocities. The black bar in Fig. 3(b) represents the contribution of the pullback factor, and the red one represents the influence of the pushout factor. Both contributions increased the ring width as the impact velocity increased, but the pullback factor played a leading role in the formation of a nonparticle disc structure and contributed to more than 90% of the disc width. The ratio remained nearly unchanged for the same reason as above within the velocity range of this experiment, as illustrated in Fig. 3(c).

Figure 4(a) shows the maximum spread distance  $D_{max}$  ( $D_{max} = 2 \times R_{max}$ ) normalized by the drop diameter  $D_0$  vs the Weber number. The maximum spread distance was greater at higher Weber numbers (higher impact velocity) due to higher drop kinetic energy and shows a scale relation  $D_{max} \sim We^{1/4}$ , for both hydrophilic and hydrophobic cases. This scaling was consistent with the previous analysis and also agreed with other research.<sup>25,31</sup> However, as the numerical values indicated,  $D_{max}$  was clearly higher in the hydrophilic surface case compared to the hydrophobic surface for almost all Weber numbers in this experiment. We attribute this to the competition of hydrophilic properties between the hydrophilic glass slide, hydrophobic glass slide, and PMMA surface, and the

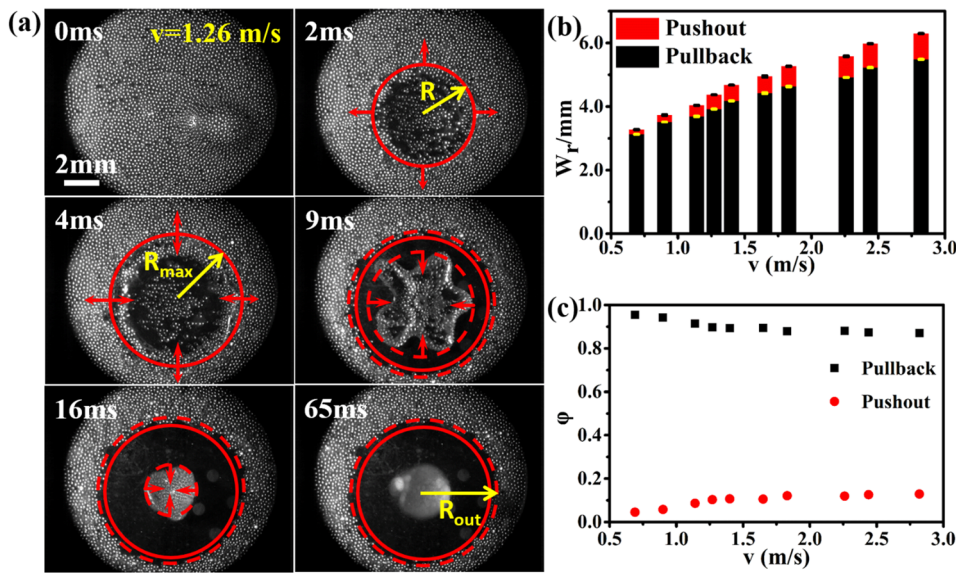


**FIG. 3.** (a) The corresponding fast speed images show the formation of the non-particle disc-like structure during drop impact on a single layer of particles on the hydrophobic surface. The red solid circle shows the drop front, which was also the contour of moving particles. Red arrows demonstrate the instantaneous position and direction of motion of the particles. (b) Plot of  $W_r$  vs  $v$  based on the contributions of the two factors, and red and black bars stand for pushout and pullback, respectively. (c) The contribution ratio of each factor on disc width is plotted for various impact velocities. Red circles and black squares represent the contribution ratios of pushout and pullback factors, respectively.

corresponding drop contact angles are shown in Figs. 4(d)–4(f). In the hydrophilic surface case, the drop preferentially contacted the glass slide over the PMMA particles, and so most particles splashed out instead of sticking when the expanding drop touched them. When a drop impacted the hydrophobic glass slide, however, it preferentially attached to particles over the hydrophobic surface, which was demonstrated by a higher drop angle of contact on the hydrophobic surface seen in Fig. 4(e), compared to the PMMA surface shown in Fig. 4(f). Thus, more particles would stick on the drop and restrict movement, leading to a lower maximum spread distance in the hydrophobic surface case.

Our experiment suggested that pushout and pullback factors can both affect the formation of the nonparticle ring/disc, and the pushout factor plays a main role when the drop hits a particle layer on a hydrophilic surface, but the pullback factor has a more significant influence during drop impacts on a hydrophobic glass slide. Figure 4(b) shows the contribution of the pushout factor on the nonparticle ring/disc width for both hydrophilic and hydrophobic surfaces.  $W_{pushout}$  had a similar trend for different surface types as the drop impact velocity increased, but had a slightly smaller value on the hydrophobic slide compared with the hydrophilic surface. This difference can also be explained by the same reason described

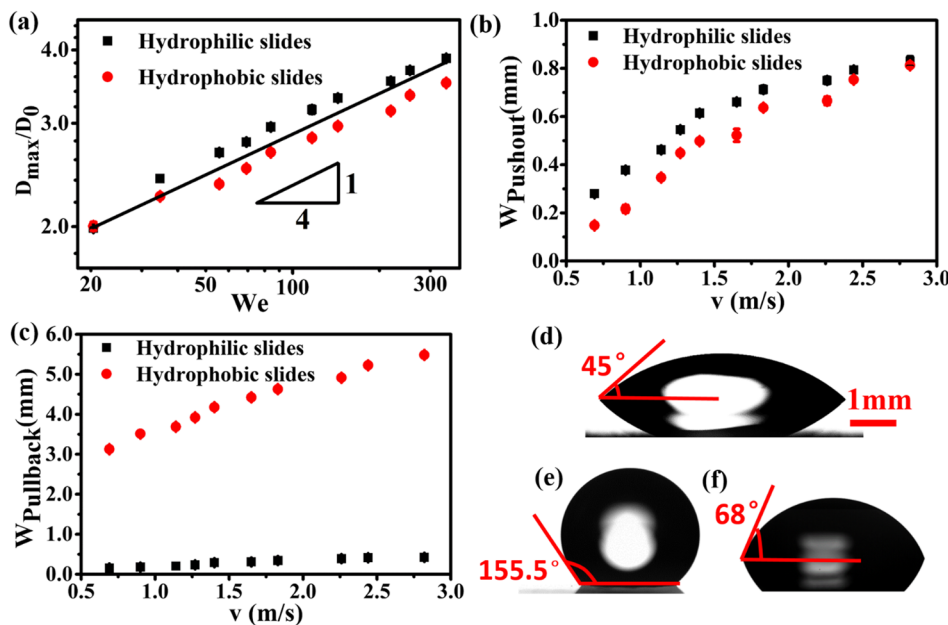


**FIG. 4.** (a) Double logarithmic plot of  $D_{max}/D_0$  vs the Weber number for hydrophilic (black squares) and hydrophobic (red circles) surfaces. (b)  $W_{pushout}$  is a function of impact velocity for hydrophilic (black squares) and hydrophobic (red circles) slides. (c)  $W_{pullback}$  is plotted as a function of impacting velocity for hydrophilic (black squares) and hydrophobic (red circles) slides. (d), (e), and (f) show the drop contact angles on the hydrophilic slide, the hydrophobic slide, and the PMMA surface, respectively.

in Fig. 4(a). The drop spread on a hydrophobic surface was subject to stronger resistance and provided less kinetic energy to the particles in front.  $W_{pullback}$  is also plotted in Fig. 4(c) for various impact velocities. It is clear that  $W_{pullback}$  was much greater in hydrophobic surface case due to the full rebound of drops on the hydrophobic slide.

## CONCLUSIONS

In this paper, we systematically studied the impacts of a water drop upon a single layer of PMMA particles on hydrophilic/hydrophobic surfaces. This study confirmed that two factors correspond to the formation of a nonparticle ring/disc. The pushout factor played a main role when the surface was hydrophilic, while when a drop hit a hydrophobic surface, the pullback factor dominated the formation of a nonparticle disc. Our scaling analysis indicated for the first time that the ratio of contribution of each factor on the ring/disc width was independent of the impact velocity, and this was also verified by our experiment. In order to explain the difference in the maximum spread distance, we compared the corresponding hydrophilic properties of a drop on a hydrophilic slide, a hydrophobic slide, and a PMMA surface. We found that the drop preferred to touch PMMA particles (lower contact angle) instead of the hydrophobic surface (higher contact angle). Thus the adhesion of more particles on the drop led to an increase in the burden of the moving drop and resulted in a lower spread distance when the drop hit the hydrophobic surface. Drop impacts are involved in many industrial and natural processes. Our experiment provided a unique perspective on nonparticle ring/disc structure formation when a drop hits a single particle layer. These findings help generalize the understanding of drop impacts on complex surfaces and could also have important practical applications in the industries related to drop impacts.

## ACKNOWLEDGMENTS

The authors are grateful for the financial support from the National Natural Science Foundation of China (Grant Nos. 11604030 and 11674043) and the Fundamental Research Funds for the Central Universities (Project Nos. 106112017CDJXY300001 and 2018CDJDWL0011).

## REFERENCES

- C. Clanet, C. Beguin, D. Richard, and D. Quere, "Maximal deformation of an impacting drop," *J. Fluid Mech.* **517**, 199 (2004).
- M. H. Klein Schaarsberg, I. R. Peters, M. Stern, K. Dodge, W. W. Zhang, and H. M. Jaeger, "From splashing to bouncing: The influence of viscosity on the impact of suspension droplets on a solid surface," *Phys. Rev. E* **93**, 062609 (2016).
- G. Riboux and J. M. Gordillo, "Experiments of drops impacting a smooth solid surface: A model of the critical impact speed for drop splashing," *Phys. Rev. Lett.* **113**, 024507 (2014).
- H. M. Huang and X. P. Chen, "Energetic analysis of drop's maximum spreading on solid surface with low impact speed," *Phys. Fluids* **30**, 022106 (2018).
- J. S. Lee, S. J. Park, J. H. Lee, B. M. Weon, K. Fezzaa, and J. H. Je, "Origin and dynamics of vortex rings in drop splashing," *Nat. Commun.* **6**, 8187 (2015).
- D. Shen, G. Zou, L. Liu, W. W. Duley, and Y. Norman Zhou, "Investigation of splashing phenomena during the impact of molten sub-micron gold droplets on solid surfaces," *Soft Matter* **12**, 295 (2016).
- J. Hao, "Effect of surface roughness on droplet splashing," *Phys. Fluids* **29**, 122105 (2017).
- A. Latka, A. M. P. Boelens, S. R. Nagel, and J. J. D. Pablo, "Drop splashing is independent of substrate wetting," *Phys. Fluids* **30**, 022105 (2018).
- J. D. Ruiters, R. Lagraauw, D. V. D. Ende, and F. Mugele, "Wettability-independent bouncing on flat surfaces mediated by thin air films," *Nat. Phys.* **11**, 48 (2015).
- C. Willis, A. K. Piranian, J. R. Donaggio, R. J. Barnett, and W. F. Rowe, "Errors in the estimation of the distance of fall and angles of impact blood drops," *Forensic Sci. Int.* **123**, 1 (2001).
- K. Clare and D. Marie, "Predicting the position of the source of blood stains for angled impacts," *J. Forensic. Sci.* **52**, 1044 (2007).
- S. Ahn, S. H. Doerr, P. Douglas, R. Bryant, C. A. E. Hamlett, G. McHale, M. I. Newton, and N. J. Shirtcliffe, "Effects of hydrophobicity on splash erosion of model soil particles by a single water drop impact," *Earth Surf. Processes Landforms* **38**, 1225 (2013).
- R. Zhao, Q. Zhang, H. Tjugito, and C. Xiang, "Raindrop impact on a sandy surface," *Phys. Fluids* **27**, 091111 (2015).
- J. B. Park, J. Y. Choi, S. H. Lee, Y. S. Song, and G. Y. Yeom, "Polymer surface texturing for direct inkjet patterning by atmospheric pressure plasma treatment," *Soft Matter* **8**, 5020 (2012).
- D. B. V. Dam and C. L. Clerc, "Experimental study of the impact of an ink-jet printed droplet on a solid substrate," *Phys. Fluids* **16**, 3403 (2004).
- K. Yong-Hoon, Y. Byungwook, J. E. Anthony, and P. Sung Kyu, "Controlled deposition of a high-performance small-molecule organic single-crystal transistor array by direct ink-jet printing," *Adv. Mater.* **24**, 497 (2012).
- A. Kumar, A. Tripathy, Y. Nam, C. Lee, and P. Sen, "Effect of geometrical parameters on rebound of impacting droplets on leaky superhydrophobic meshes," *Soft Matter* **14**, 1571 (2018).
- M. Muschi, B. Brudieu, J. Teisseire, and A. Sauret, "Drop impact dynamics on slippery liquid-infused porous surfaces: Influence of oil thickness," *Soft Matter* **14**, 1100 (2018).
- T. Supakar, M. Moradiafrapoli, G. F. Christopher, and J. O. Marston, "Spreading, encapsulation and transition to arrested shapes during drop impact onto hydrophobic powders," *J. Colloid Interface Sci.* **468**, 10 (2016).
- Z. Rui, S. Farokhirad, T. Lee, and J. Koplik, "Multiscale liquid drop impact on wettable and textured surfaces," *Phys. Fluids* **26**, 082003 (2014).
- X. Tang, A. Saha, C. K. Law, and C. Sun, "Bouncing drop on liquid film: Dynamics of interfacial gas layer," *Phys. Fluids* **31**, 013304 (2019).
- I. R. Peters, X. Qin, and H. M. Jaeger, "Splashing onset in dense suspension droplets," *Phys. Rev. Lett.* **111**, 028301 (2013).
- V. Grishaev, C. S. Iorio, F. Dubois, and A. Amirfazli, "Complex drop impact morphology," *Langmuir* **31**, 9833 (2015).
- V. Vaikuntanathan and D. Sivakumar, "Maximum spreading of liquid drops impacting on groove-textured surfaces: Effect of surface texture," *Langmuir* **32**, 2399 (2016).
- S. C. Zhao, R. de Jong, and D. van der Meer, "Raindrop impact on sand: A dynamic explanation of crater morphologies," *Soft Matter* **11**, 6562 (2015).
- M. Nicolas, "Spreading of a drop of neutrally buoyant suspension," *J. Fluid Mech.* **545**, 271 (2005).
- R. Kai and F. Feuillebois, "Influence of surface roughness on liquid drop impact," *J. Colloid Interface Sci.* **203**, 16 (1998).
- I. U. Vakarelski, N. A. Patankar, J. O. Marston, D. Y. Chan, and S. T. Thoroddsen, "Stabilization of Leidenfrost vapour layer by textured superhydrophobic surfaces," *Nature* **489**, 274 (2012).
- L. Xu, W. W. Zhang, and S. R. Nagel, "Drop splashing on a dry smooth surface," *Phys. Rev. Lett.* **94**, 184505 (2005).
- J. C. Bird, D. Rajeev, K. Hyuk-Min, and K. K. Varanasi, "Reducing the contact time of a bouncing drop," *Nature* **503**, 385 (2013).
- D. Liu, H. W. Tan, and T. Tran, "Droplet impact on heated powder bed," *Soft Matter* **14**, 9967 (2018).